ORGANOMETALLICS

Article

pubs.acs.org/Organometallics

Coordination Chemistry of Disilylated Germylenes with Group 4 Metallocenes

Johann Hlina, Judith Baumgartner,* and Christoph Marschner*

Institut für Anorganische Chemie, Technische Universität Graz, Stremayrgasse 9, 8010 Graz, Austria

Patrick Zark and Thomas Müller*

Institut für Chemie, Carl von Ossietzky Universität Oldenburg, Carl von Ossietzky-Straße 9-11, 26111 Oldenburg, Federal Republic of Germany

Supporting Information

ABSTRACT: Reaction of the PEt_3 adduct of a disilylated five-membered cyclic germylene with group 4 metallocene dichlorides in the presence of magnesium led to the formation of the respective germylene metallocene phosphine complexes of titanium, zirconium, and hafnium. Attempts to react the related NHC adduct of a disilylated four-membered cyclic germylene under the same conditions with Cp_2TiCl_2 did not give the expected germylene NHC titanocene complex. This complex was, however, obtained in the reaction of Cp_2Ti(btmsa) with the NHC germylene adduct. A computational analysis of the structure of the group 4 metallocene germylene complexes revealed the multiple-bond character of the M−Ge(II) linkage, which can be rationalized with the classical σ-donor/π-acceptor interaction. The strength of the M−Ge(II) bond increases descending group 4.

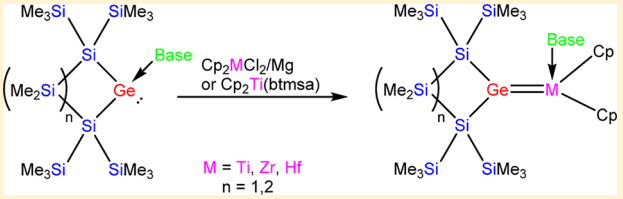

INTRODUCTION

Compared to the elements silicon and tin, the chemistry of germanium has always suffered from some neglect. The reasons for this neglect may come from commercial considerations (while Si and Sn reagents are very reasonably priced, analogous Ge compounds are quite costly) or from the lack of a spin 1/2 nucleus, which makes NMR spectroscopic analysis of organogermanium compounds difficult. As a consequence, the coordination chemistry of germanium with transition metals in general and in particular the respective chemistry of divalent Ge compounds are still not very well established[1−4] and thus require further investigations.[5] The chemistry of group 4 metallocenes with germanium-containing substituents is somewhat developed;[6−18] however, chemistry involving coordination of germylenes has so far been barely addressed.[19]

In the course of our studies concerning silyl-substituted tetrylenes we have recently reported the reactions of a 1,4-oligosilanyl dianion[20,21] with $PbBr_2$, $SnCl_2$, and $GeCl_2$ in the presence of PEt_3 to phosphine adducts of the respective cyclic plumbylene,[22] stannylene,[23] and germylene.[24] In a subsequent contribution we demonstrated that the dimeric forms of these plumbylene and stannylene but also the respective PEt_3 adducts could be used to obtain group 4 metallocene plumbylene and stannylene complexes **I** and **II**.[25]

The synthesis of the stannylene complexes was not completely unexpected, as we had previously observed the intermediate formation of related complexes during attempts to prepare group 4 metallocene distannene complexes.[6] However, the same study also addressed the formation of group 4 metallocene digermene complexes, which were found to be stable compounds.

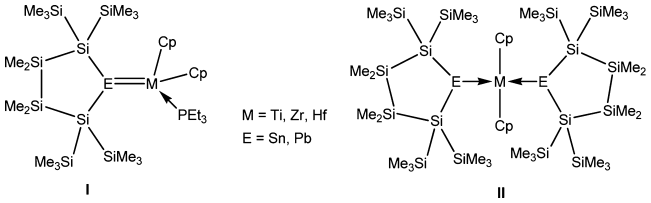

I II

Group 4 metallocene complexes of the higher tetrylenes are not very abundant in general. In addition to our recently reported stannylene and plumbylene compounds[25] also a few other zirconocene stannylene complexes,[26−28] two recently reported examples of titanocene silylene complexes,[29,30] and an example of a silylene hafnocene complex[31] are known.

With the recent availability of germylene phosphine adducts[24] the question arose whether the addition of disilylated germylenes to group 4 metallocenes would lead to the respective germylene or digermene complexes.

RESULTS AND DISCUSSION

Synthesis. Reduction of group 4 metallocene dichlorides with magnesium[25,32,33] in the presence of the germylene PEt_3 adduct **1**[24] in THF gave the respective metallocene germylene complexes of titanocene, zirconocene, and hafnocene as PEt_3 adducts (**2**−**4**) (Scheme 1).

When we recently tried to vary the chemistry of cyclic disilylated germylenes, we found that a compound analogous to

Received: March 14, 2013
Published: May 17, 2013

   dx.doi.org/10.1021/om400215v | *Organometallics* 2013, 32, 3300−3308

Scheme 1. Formation of Group 4 Metallocene Germylene Complex Base Adducts (2−4 and 2a)

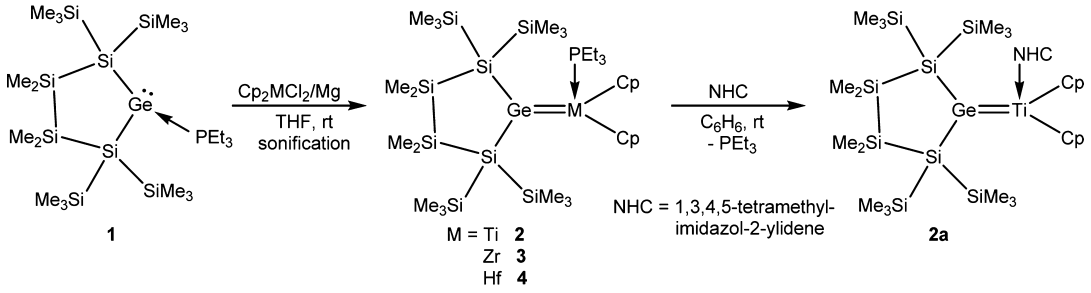

1 but with the divalent Ge atom embedded into a four-membered ring could be prepared.[34] This adduct was however less stable, and the behavior of the respective free germylene was strongly different from the germylene released from **1**.[34] It was therefore of interest to study whether this particular germylene could be used to form complexes analogous to **2**−**4**. As the germylene incorporated in the four-membered ring was not sufficiently stabilized with PEt_3, it was isolated as a 1,3,4,5-tetramethylimidazol-2-ylidene (NHC) adduct (**5**). Unfortunately, attempts to react **5** with the Cp_2TiCl_2/magnesium system did not give the expected titanocene germylene complex **6**. However, when **5** was reacted with Rosenthal's "Cp_2Ti" precursor[35,36] $Cp_2Ti(btmsa)$[32] at slightly elevated temperature, a smooth conversion to the titanocene germylene NHC adduct **6** occurred (Scheme 2). The same route was demonstrated to be suitable also

Scheme 2. Alternative Procedure for the Formation of Group 4 Metallocene Germylene Complexes

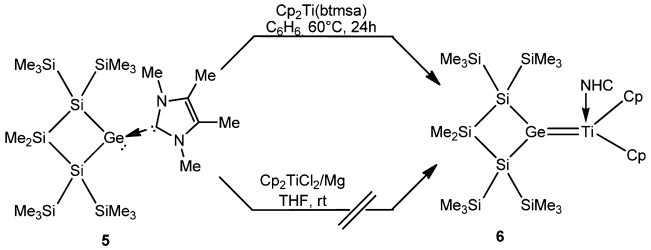

for the preparation of the phosphine complexes. Reaction of $Cp_2Ti(btmsa)$ with **1** in C_6H_6 thus provided an alternative way to complex **2**. To obtain a titanocene complex with the germylene derived from **1** and the NHC present in **5**, compound **2** was reacted with the respective NHC in benzene to give compound **2a**, in which the PEt_3 ligand is replaced by the NHC (Scheme 1).

Crystal Structure Analysis. Molecular structures of all germylene PEt_3 complexes [**2**, **3**, **4** (Figure 1), and **6** (Figure 2)] in the solid state could be determined by means of single-crystal X-ray diffraction. All complexes feature the Ge atom in the metallocene's equatorial plane and the five-membered ring orientated in an almost orthogonal way to this plane. The same arrangement was also observed for the analogous stannylene and plumbylene complexes[25] and also for Sekiguchi's hafnocene and titanocene silylene complexes,[30,31] which were isolated as a PMe_3, THF, or isonitrile adducts. This particular conformation seems to guarantee good orbital overlap between the metal's filled d-orbitals and the empty germylene p-orbital. The recently reported titanocene disilylene complexes by Blom et al.[29] also exhibit this conformation, although the base stabilization of the empty silylene orbital in these complexes should actually weaken the interaction with the metal's filled d-orbitals. For compounds **2**, **3**, and **4** the PEt_3 ligands are situated also in the metallocenes' equatorial planes at an angle of 90° to the germanium atom. The 90° angle was also observed for all examples of the recently reported stannylene and plumbylene complexes and shows a nondisturbance of the Ge−transition metal interaction by the orthogonal phosphine ligand.[25] For the NHC complex **6** the situation is similar, but in addition the NHC features a particular orientation that is in plane with the metallocene's equatorial plane. A search for comparable group 4 metallocenes with coordinated NHCs surprisingly reveals only very few compounds.[37−39] However, all of these feature the NHC plane in the equatorial plane of the metallocene. Erker, Berke, and co-workers[37] found this behavior for group 4 metallocene cations. In their quest for an explanation for this unusual conformational property, they conducted DFT calculations to detect interactions exceeding exclusive σ-donor behavior of the NHC. Their conclusion eventually was that the restricted rotation of the (larger) NHC is based on steric grounds.[37] With the evidence of other reports[38,39] and the behavior of **6** the question arises whether this explanation may not be too simple.

The asymmetric unit of **6** contains two molecules of the complex in addition to two molecules of benzene. Comparison of the Ge-group 4 element bond lengths with known examples is not straightforward, as structurally characterized compounds featuring this type of bond are quite rare. The two reported compounds with Ge−Ti bonds $(Me_3Si)_3Ge-Ti(NMe_2)_3$ (2.653 Å)[9,40] and $Ph_3Ge-TiCp_2(COMe)$ (2.710 Å)[13] exhibit considerably longer bonds compared to the 2.536 Å for **2** and 2.522 Å for **6**, which again strongly supports the notion of a bond order higher than one between the metal and the germylene. The only reported example of a structurally characterized molecule containing a zirconocene−germanium bond is the PMe_3 adduct of a digermene zirconocene complex,[6] with Ge−Zr bond distances of 2.870 and 2.913 Å. The analogous hafnocene complex[6] features Hf−Ge distances of 2.867 and 2.841 Å, while the Ge−Hf distance of an analogous silagermene hafnocene complex[6] is 2.837 Å. In comparison to these values the Hf−Ge bond of $Cp^*HfCl_2Ge(SiMe_3)_3$[12] is shorter (2.790 Å). However, all these bond lengths are clearly longer than the Zr/Hf−Ge distances of **3** (2.632 Å) and **4** (2.600 Å), indicating again multiple-bond character.

The distances between the germylene atom and the attached silicon atoms are also affected by the coordination to the metal. While bond distances of 2.427 and 2.446 Å[24] were observed for the PEt_3 adduct **1**, the respective metallocene-coordinated compounds feature distances of 2.475/2.468 Å for **2**, 2.465/2.458 Å for **3**, and 2.460/2.455 Å for **4**. It remains, however, open to discussion how valid such a correlation is since an NHC-coordinated analogue of **1** displays Ge−Si distances of 2.471 and 2.479 Å.[24]

NMR Spectroscopy. While the bonding situation of the group 4 metallocene stannylene and plumbylene complexes[25]

dx.doi.org/10.1021/om400215v | Organometallics 2013, 32, 3300−3308

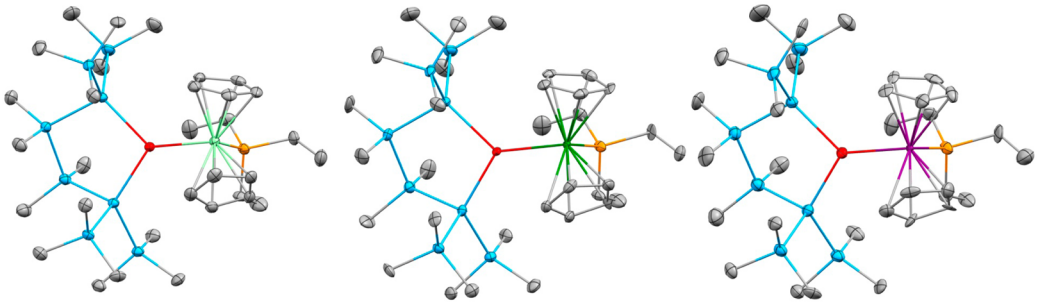

2	3	4
dark blue crystals	dark purple crystals	dark purple crystals
space group: P-1	space group: P-1	space group: P-1
Ge-Ti: 253.6(1) pm	Ge-Zr: 263.2(1) pm	Ge-Hf: 260.0(1) pm
$\sum r_{cov}$ (Ge/Ti) 254 pm	$\sum r_{cov}$ (Ge/Zr) 267 pm	$\sum r_{cov}$(Ge/Hf) 266 pm
Ge-Si: 246.8(1) / 247.5(1) pm	Ge-Si: 245.9(2) / 246.5(3) pm	Ge-Si:245.4(4) / 246.0(4) pm
Si-Ge-Si: 101.8(1)°	Si-Ge-Si: 101.79(8)°	Si-Ge-Si 101.8(1)°
Si-Ge-Ti: 128.15(3) / 129.93(4)°	Si-Ge-Zr: 128.46(7) / 129.34(7)°	Si-Ge-Zr: 128.6(1) / 129.2(1)°
Ge-Ti-P: 90.91(3)°	Ge-Zr-P: 91.79(6)°	Ge-Hf-P: 92.13(9)°

Figure 1. Crystal structures of **2**, **3**, and **4**. Thermal ellipsoids are at the 30% probability level, and hydrogen atoms are omitted for clarity.

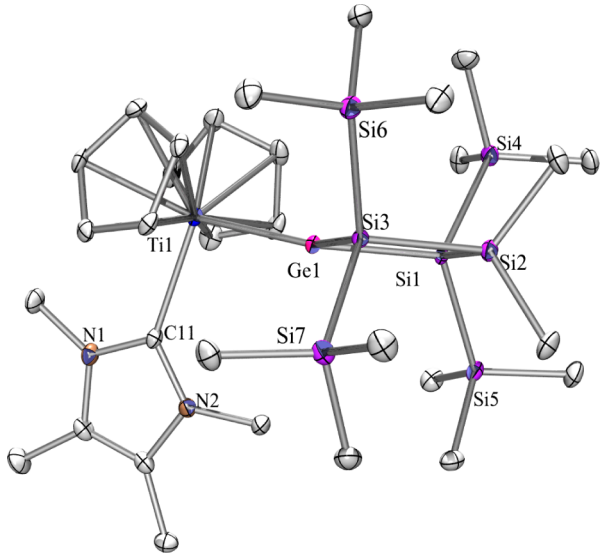

Figure 2. Crystal structure of **6**. Thermal ellipsoids are represented at the 30% level, and hydrogen atoms have been omitted for clarity. Bond lengths (Å) and angles (deg): Ti(1)−C(11) 2.323(2), Ti(1)−Ge(1) 2.5217(8), Ge(1)−Si(3) 2.4465(9), Ge(1)−Si(1) 2.4567(8), Si(1)−Si(2) 2.3628(10), Si(2)−C(18) 1.883(2), N(1)−C(11) 1.371(3), C(11)−Ti(1)−Ge(1) 102.82(6), Si(3)−Ge(1)−Si(1) 87.27(3), N(1)−C(11)−N(2) 101.62(19).

could be analyzed very well by means of ^{119}Sn and ^{207}Pb NMR spectroscopy, this is not as easily possible for the analogous germylene complexes, as germanium does not possess advantageous NMR properties. However, comparison of ^{1}H, ^{13}C, ^{29}Si, and ^{31}P spectra provides nevertheless some insight into the properties of these compounds.

While the structural properties of compounds **2**−**4** are quite similar, with respect to the NMR spectroscopic features the titanocene complex **2** is somewhat different from **3** and **4**. At ambient temperature the ^{29}Si spectrum of **2** exhibits only a very broad signal for the trimethylsilyl groups, which becomes a sharp peak when raising the temperature to 50 °C. Together with the fact that the ambient temperature ^{29}Si NMR spectra of **3** and **4** show two signals for the trimethylsilyl groups, this strongly indicates that the multiple-bond character of the Ge−Ti bond is not high enough to suppress rotation around this bond at room temperature. To rule out the decomplexation/complexation behavior of PEt_3 as the reason for the observed dynamic process, NMR spectra of compound **2** were measured in the presence of an excess of PEt_3 to suppress a possible decomplexation step. However, no change in the appearance of the spectra was observed.

For compounds **3** and **4** two different signals for the trimethylsilyl groups on different sides of the ring were observed, both of which also featured couplings to the PEt_3 phosphorus atom. Compared to the germylene phosphine adduct **1**, which exhibits the ^{29}Si NMR resonance for the atoms attached directly to germanium at δ = −127.1 ppm, the analogous signals for the complexed germylenes **2**, **3**, and **4** are shifted downfield by almost 30 ppm and were found for all complexes close to −100 ppm. The ^{31}P chemical shift is of course more sensitive to a change of metal, and the respective resonances of the three complexes were found at δ = 42.9 (**2**), 31.0 (**3**), and 28.4 ppm (**4**).

The exchange of PEt_3 for 1,3,4,5-tetramethylimidazol-2-ylidene to obtain **2a** caused a change in the ^{29}Si spectroscopic behavior so that two different resonances for the trimethylsilyl groups can be observed at ambient temperature. However, the reason for this behavior seems not to be a higher degree of Ge−Ti bond order but rather a steric interaction between the cyclic germylene and the coordinated NHC. The ^{1}H and ^{13}C methyl resonances of the NHC also exhibit a side differentiation for the two hemispheres of the heterocycle. Thus also the rotation around the Ti−C bond seems to be restricted. NOE studies allowed assignment of the NHC's four methyl groups.

The ^{13}C NMR resonance of the carbene carbon atom of **2a** was found at 198.2 ppm, compared to the free NHC resonance at 212.7 ppm.[41] For the related complex **6** the spectroscopic picture is similar to **2a**. Compared to **2**, **3**, and **4** the ^{29}Si NMR resonance for the atoms attached to the germanium atom is shifted some 30 ppm to lower field (δ = −68.7 ppm), which is a typical effect for atoms incorporated into a four-membered ring.

dx.doi.org/10.1021/om400215v | *Organometallics* 2013, 32, 3300−3308

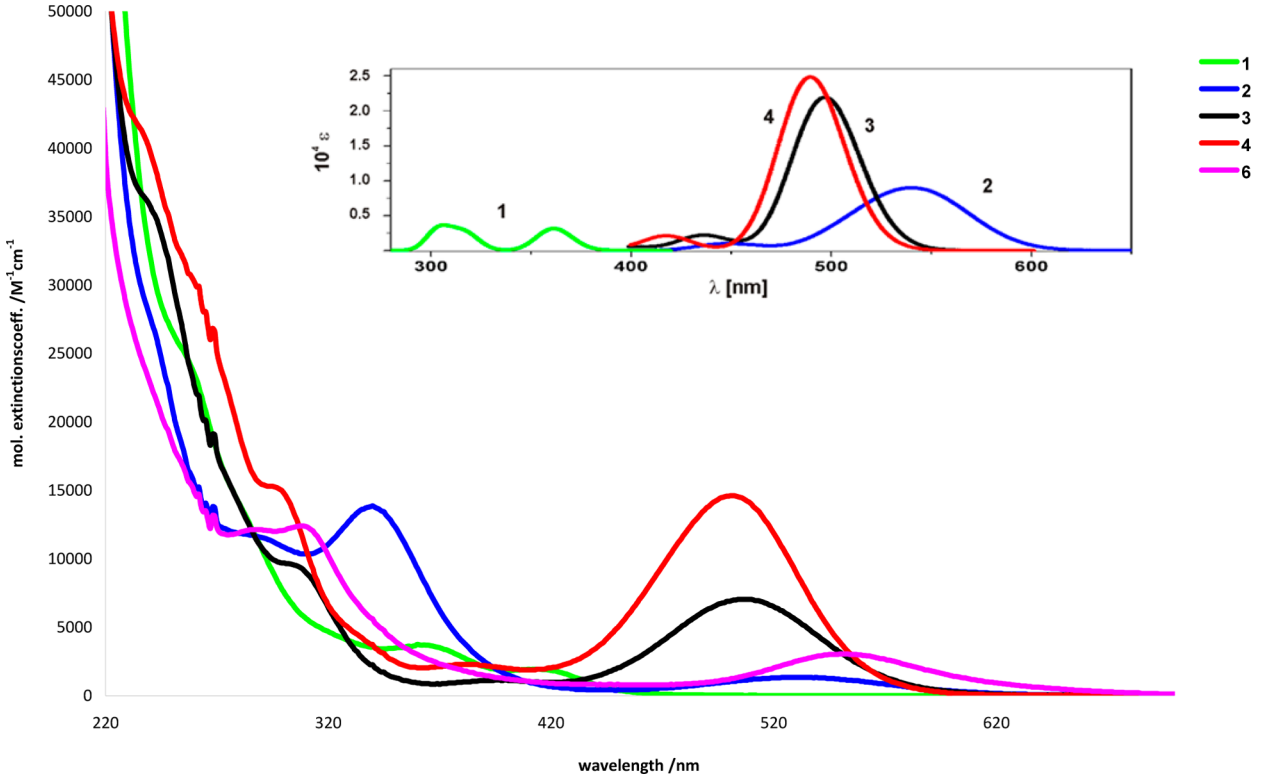

Figure 3. UV/vis spectra of compounds **1**–**4** and **6**. Inset: Calculated UV spectra for compounds **1**–**4** (TD/B3LYP/def2-tzvp//M06-2X/SDD(Ge,Ti,Zr,Hf), 6-31G(d)(P,Si,C,H)). The line shape of the theoretical spectra was simulated with a Lorentzian function with a half line width of 124 nm (0.1 eV).

With only 0.3 ppm the difference in the chemical shifts of the two sets of different trimethylsilyl groups of **6** is considerably smaller than what was found for **2a**, which suggests less steric interaction with the NHC. Also the ^{13}C chemical shift of the coordinating carbene atom (δ = 197.6 ppm) is almost identical to the one found for **2a**. NOE studies allowed assignment of the NHC resonances and in addition also showed that the rotation around the Ti–Ge bond is not completely restricted.

UV/Vis Spectroscopy. Compared to the PEt_3 adduct of the free germylene (**1**) the UV/vis spectra of compounds **2**, **3**, **4**, and **6** all display a bathochromic shift of the lowest energy band (Figure 3). Titanocene compound **2** exhibits a shoulder around 288 nm ($\varepsilon = 1.2 \times 10^4$ L mol^{-1} cm^{-1}) and a band at 340 nm ($\varepsilon = 1.4 \times 10^4$ L mol^{-1} cm^{-1}) in addition to another band at 531 nm ($\varepsilon = 1.3 \times 10^3$ L mol^{-1} cm^{-1}), which is responsible for the deep violet to blue color of the solution. Zirconocene **3** features a shoulder close to 302 nm ($\varepsilon = 9.5 \times 10^3$ L mol^{-1} cm^{-1}) and a weak band at 400 nm ($\varepsilon = 1.1 \times 10^3$ L mol^{-1} cm^{-1}). The lowest energy band of **3** with a maximum at 507 nm ($\varepsilon = 7.0 \times 10^3$ L mol^{-1} cm^{-1}) is hypsochromically shifted compared to **2** but shows a stronger degree of absorption. The color of **3**, being deep red to violet, differs from **2**. As frequently observed, the hafnium compound **4** shows a stronger similarity to the analogous zirconium complex than to the titanium congener. Besides the shoulder at 294 nm ($\varepsilon = 1.5 \times 10^4$ L mol^{-1} cm^{-1}) the absorption bands at 382 nm ($\varepsilon = 2.3 \times 10^3$ L mol^{-1} cm^{-1}) and 502 nm ($\varepsilon = 1.5 \times 10^4$ L mol^{-1} cm^{-1}) are close to those of **3**, as is the color. Titanocene derivative **6**, which carries the NHC instead of the PEt_3 as base and a germylene incorporated into a four-membered ring, exhibits a different absorption behavior compared to titanocene complex **2**. Two close bands were detected at 288 nm ($\varepsilon = 1.2 \times 10^4$ L mol^{-1} cm^{-1}) and 308 nm ($\varepsilon = 1.2 \times 10^4$ L mol^{-1} cm^{-1}). The lowest energy band of **6** at 552 nm ($\varepsilon = 3.1 \times 10^3$ L mol^{-1} cm^{-1}) has the highest bathochromic shift of all compounds described here. Its solution thus exhibits a deep violet to blue color. TD-DFT calculations[42] predict for compounds **2**–**4** electronic absorption spectra that are very close to those experimentally observed. (λ_{max}: 540 nm (**2**), 497 nm (**3**), 490 nm (**4**); see Figure 3 and the Supporting Information). In the case of the zirconium and hafnium metallocenes the long wave transition can be associated with the $\pi \rightarrow \pi^*$ transition of the M–Ge bond. For the titanium compound **2** the situation is less clear, as two energetically contiguous exited states contribute to the observed broad absorption band. Both calculated absorption maxima result from $\pi \rightarrow \pi^*$ and $\pi \rightarrow \sigma^*$ transitions with maxima at 529 nm and at 555 nm. By applying a natural line width of 124 nm both individual bands merge into a broad absorption with a maximum at 540 nm.

Theoretical Studies.[42] Optimization of the molecular structures of the group 4 element germylene complexes **2**–**4** at the density functional M06-2X/SDD (Ge, Ti, Zr, Hf), 6-31G(d) (P, Si, C, H) level of theory results in structural parameters that are very close to those found by X-ray diffraction methods for these compounds. Data important for the discussion are summarized in Table 1. For germylene **7**, for which no experimental structural data are available, a half-chair conformation of the metallacyclopentasilane ring was predicted with the germanium atom and the two neighboring silicon atoms spanning the central plane.[43] A common feature of the optimized molecular structures of germylene complexes **2**–**4** are trigonal planar coordinated Ge atoms (sum of the bond angles α around the germanium atom, $\sum\alpha$(Ge) = 358.9–359.4°) embedded in a half-chair germacyclopentasilane ring of local C_2 symmetry. The

dx.doi.org/10.1021/om400215v | *Organometallics* 2013, 32, 3300–3308

Table 1. Selected Experimental and Calculated [in parentheses, at M06-2X/SDD (M,E), 6-31G(d) (Si,C,H)] Structural Parameter, Wiberg Bond Indices (WBI), and Molecular Orbital Energy Differences ΔE for Germylene 7 and Germylene Complexes 2−4 of Group 4 Metallocenes[a]

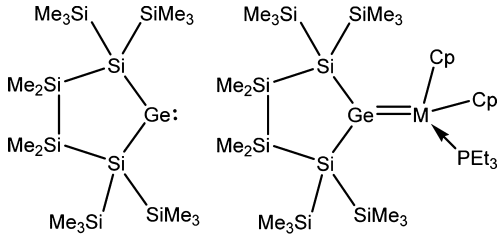

7

M | Ti | Zr | Hf
2 | 3 | 4

cpd	M/E	d(M−Ge) [pm]	d(Ge−Si) [pm]	α(Ge,M,P) [deg]	α(Si,Ge,Si) [deg]	WBI (MGe)	$\Delta E(d_{xz}/\pi)^b$ [eV]	$\Delta E(p_x/\pi^*)^b$ [eV]	ΔE(HOMO/LUMO) [eV]	BDE (MGe) [kJ mol^{-1}]	BDE^{B3LYP} (MGe) [kJ mol^{-1}]	BDE^{NCI} (MGe) [kJ mol^{-1}]
2	Ti/Ge	253.6 (249.2)	247.2 (251.3)	90.9 (91.0)	101.4 (100.3)	1.54	0.39	1.13	4.38	177	80	97
3	Zr/Ge	263.2 (261.8)	247.7 (249.0)	91.8 (93.3)	101.8 (101.6)	1.66	0.72	1.33	4.33	276	174	102
4	Hf/Ge	260.0 (262.0)	245.7 (248.3)	92.1 (93.3)	101.8 (102.0)	1.64	0.80	1.47	4.35	300	194	126
7	−/Ge		(248.0)		(93.5)							

[a]Bond dissociation energies (BDE) of the MGe bonds calculated using the M06-2X functional are given as BDE(MGe). For comparison, the BDE computed applying the B3LYP functional, here denoted as BDE^{B3LYP}(MGe), are summarized as well. Finally, the noncovalent contributions to the BDE, BDE^{NCI}(MGe), calculated from the difference between BDE(MGe) and BDE^{B3LYP}(MGe) are listed. [b]For definition see Figure 4.

dx.doi.org/10.1021/om400215v | *Organometallics* 2013, 32, 3300−3308

computational results indicate no significant influence of the complexation on the molecular structure of the germylene **7**. The most obvious structural modification is a widening of the endocyclic SiGeSi bond angle α(SiGeSi) by 6.8−8.5° (see Table 1). In accordance with the experimental structures, the results of the computation predict that the germylene units are oriented mostly perpendicular to the central Ge−M−P plane in tetrylene complexes **2**−**4** (dihedral angle β = 82−83°).[44] This specific arrangement allows for an efficient back-bonding from metal d-orbitals to the formally empty p-orbital at the germanium atom. The calculated M−Ge(II) bond lengths, which are summarized in Table 1, show the expected trends. That is, the Ge−M distance increases from the Ge/Ti to Ge/Zr, and it remains constant when the zirconocene germylene complex is compared to the hafnocene complex. The calculated M−Ge(II) bond lengths as well as those determined experimentally (see Table 1) are all smaller than standard values for E−M single bonds (Ge−M: 257 pm (Ti), 275 pm (Zr), 273 pm (Hf));[45] in no case, however, are the values predicted for $\sigma^2\pi^2$ Ge═M double bonds reached (Ge═M: 228 pm (Ti), 238 pm (Zr), 239 pm (Hf)).[45] In agreement with these structural criteria also the results of a natural bond orbital (NBO) analysis indicate the multiple-bond character for the M−Ge(II) linkage in germylene complexes **2**−**4** (see Table 1). In detail, all calculated Wiberg bond indices (WBIs) are significantly larger than computed for the respective M−Ge(IV) single bond in the corresponding metallocene-digermyl compound ($Cp_2M(GeMe_3)_2$) [WBI: 0.83 (Ti−Ge), 0.92 (Zr−Ge), 0.92 (Hf−Ge)]. The calculated bond orders for the M−Ge(II) bond, as expressed by the WBIs, increase in the order Ti < Zr ≈ Hf. This trend is also reflected by the computed bond dissociation energies for the metal−germanium bond BDE(MGe) for the germylene complexes (see Table 1). The Ge(II)−Ti bond is significantly less stable than the Ge(II)−Zr bonds [by 99 kJ mol^{-1}], and there is a second although smaller increase predicted for the BDE of the Ge(II)−Hf bonds (by 24 kJ mol^{-1}).

The bonding between the zirconium and the germanium atom in the germylene complex **3** is rationalized by the orbital interaction diagram shown in Figure 4. Plots of the surface

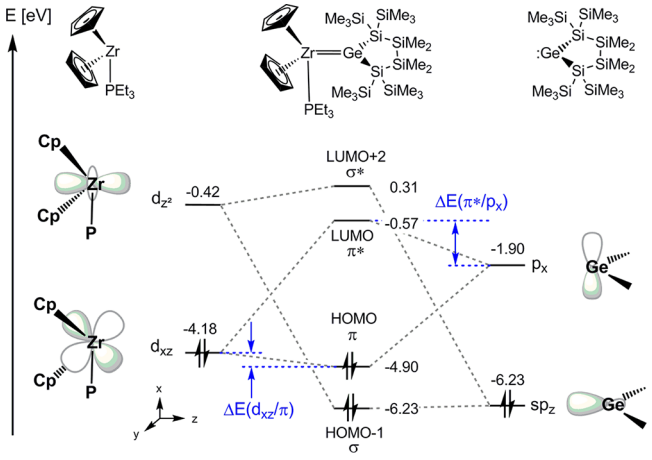

Figure 4. FMO interaction scheme for germylene complex **3**, derived from M06-2X/SDD (Zr,Ge), 6-31G(d) (P, Si, C, H) calculations. This MO scheme is qualitatively also valid for the germylene complexes **2** and **4**.

diagrams for frontier molecular orbitals of compound **3** can be found in the Supporting Information. The M−Ge(II) bond in complexes **2**−**4** is best described by the conventional σ-bonding/(d/p) π-back-bonding scheme for carbene complexes. In the framework of perturbation theory, the relative extent of back-bonding in the metallocene germylene complex can be estimated by the evaluation of the calculated orbital stabilization energy $\Delta E(d_{xz}/\pi)$ and the corresponding destabilization energy $\Delta E(\pi^*/p_x)$ (see Figure 4 and Table 1). Both energy differences increase for metallocene germylene complexes along the series Ti < Zr < Hf. This suggests that the $d_{xz} \rightarrow p_x$ π-back-bonding is smallest for the titanium complex **2** and largest for the hafnium compound **4**. This graded order of π-back-bonding mirrors the dynamic NMR properties of the titanium complex **2** compared to its hafnium and zirconium congeners.

The relative weakness of the germanium−titanium bond in compound **2** is a result of two facts. There is the well-known phenomenon that single bonds between 3d transition metals and ligands are weaker than between 4d and 5d metals and the same ligand. This is rationalized by the similar size of 3d and occupied 3p shells and the resulting Pauli repulsion between the occupied 3p orbitals and donor orbitals of the ligand.[46,47] In transition metal complexes with pronounced back-bonding the metal−ligand binding energy can be larger for 3d metals than for 4d metals. A V-like trend of the binding energy results; that is, 5d > 3d > 4d.[48,49] In these cases the relative energies of metal and ligand orbitals involved in back-bonding is of importance. We noted already the poor ability of the titanocene to engage in π-bonding. This is mostly due to the poor spatial and energetic match between the $3d_{xz}$-orbital of titanium and the $4p_x$-orbital of the germanium atom ($\Delta E(d_{xz}/p_x)$ = 2.86 eV vs 2.28 eV for Zr or 2.09 eV for Hf).

A short comparison to the recently investigated analogous group 4 metallocene stannylene and plumbylene complexes[22] is here appropriate. As expected, the strength of the E(II)/M bond in tetrylene complexes for a given group 4 metallocene as gauged by their calculated BDEs decreases along the series of group 14 elements (BDE(Ti−E): 177 kJ mol^{-1} (Ge), 151 kJ mol^{-1} (Sn), 118 kJ mol^{-1} (Pb); BDE(Zr−E): 276 kJ mol^{-1} (Ge), 249 kJ mol^{-1} (Sn), 215 kJ mol^{-1} (Pb); BDE(Hf−E): 300 kJ mol^{-1} (Ge), 270 kJ mol^{-1} (Sn), 234 kJ mol^{-1} (Pb)).[22] Consequently the results of the calculations predict group 4 metallocenes with the cyclic persilylated silylene as the partner complexes with the strongest M−E bonds in this series (BDE(M−Si): 209 kJ mol^{-1} (Ti), 311 kJ mol^{-1} (Zr), 337 kJ mol^{-1} (Hf)).[50] These results suggest that also the corresponding silylene group 14 metallocene complexes are viable targets for synthesis.

The large and polarizable substituents that are present in all three investigated metallocene complexes suggest that attractive dispersion energy contributions to the overall binding energy of the complexes might be a decisive factor. The here applied M06-2X functional[51] properly accounts for dispersion forces, while the most prominent deficit of the popular B3LYP functional is the nearly complete negligence of noncovalent van der Waals interactions. Therefore, the difference in the calculated bond dissociation energies (BDEs) using these two functionals allows estimating the contribution of noncovalent bonding in metallocene complexes **2**−**4**.[22,25,52−54] The contribution of noncovalent interactions, BDE^{NCI}, to the overall BDE, which is calculated as the difference between the BDE obtained at the M06-2X level and the reduced BDE^{B3LYP} obtained at the B3LYP level (see Table 1), is substantial in all cases. In the case of the titanium complexes it accounts for 55% of the overall BDE, and even in the hafnium complexes it amounts to 42%.

dx.doi.org/10.1021/om400215v | Organometallics 2013, 32, 3300−3308

CONCLUSION

In order to study the chemistry of group 4 metallocene germylene complexes, reactions of the PEt_3 adduct of a disilylated five-membered cyclic germylene with group 4 metallocene dichlorides in the presence of magnesium were carried out. The formation of the respective germylene metallocene phosphine complexes of titanium, zirconium, and hafnium proceeded similarly to that in a previously reported study on analogous stannylene and plumbylene complexes.[25]

NMR spectroscopic and crystallographic evidence for a multiple-bond character between the transition metal and germanium was supported by a theoretical study.

In addition to the complexes with disilylated five-membered cyclic germylenes also an example with a smaller ring was prepared. Since the PEt_3 adduct of the respective precursor for this compound proved to be unstable, related NHC-coordinated germylene was utilized to serve as starting material in the reactions with $Cp_2Ti(btmsa)$.

Group 4 metallocene complexes of heavy carbene analogues have not been very well studied so far. Despite the fact that recently several examples of silylene complexes of group 4 metallocenes[29−31] were reported and a couple of stannylene[25−28] and plumbylene[25] complexes are known, we think that to the best of our knowledge the compounds in the current account represent the first published[19] examples of germylene complexes of this group.

EXPERIMENTAL SECTION

General Remarks. All reactions involving air-sensitive compounds were carried out under an atmosphere of dry nitrogen or argon using either Schlenk techniques or a glovebox. All solvents were dried using a column-based solvent purification system.[55] If not noted otherwise, all chemicals were obtained from different suppliers and used without further purification.

^1H (300 MHz), ^{13}C (75.4 MHz), ^{31}P (124.4 MHz), and ^{29}Si (59.3 MHz) NMR spectra were recorded on a Varian INOVA 300 spectrometer, and C_6D_6 was used as solvent. To compensate for the low isotopic abundance of ^{29}Si, the INEPT pulse sequence[56,57] was used for the amplification of the signal.

Crystal Structure Determination. For X-ray structure analyses the crystals were mounted onto the tip of glass fibers, and data collection was performed with a Bruker-AXS SMART APEX CCD diffractometer using graphite-monochromated Mo Kα radiation (0.71073 Å). The data were reduced to F_o^2 and corrected for absorption effects with SAINT[58] and SADABS,[59,60] respectively. The structures were solved by direct methods and refined by the full-matrix least-squares method (SHELXL97).[61] Non-hydrogen atoms were refined with anisotropic displacement parameters, and hydrogen atoms were located in calculated positions to correspond to standard bond lengths and angles. Unfortunately the obtained crystal quality of some substances was poor. This fact is reflected by quite high R and low theta values.

Crystallographic data (excluding structure factors) for the structures of compounds **2**, **3**, **4**, and **6** reported in this paper have been deposited with the Cambridge Crystallographic Data Center as supplementary publication nos. CCDC-881603 (**2**), 881604 (**3**), 881605 (**4**), and 881606 (**6**). Copies of data can be obtained free of charge at http://www.ccdc.cam.ac.uk/products/csd/request/.

Compounds **1**,[24] $Cp_2Ti(btmsa)$,[32] 1,3,4,5-tetramethylimidazol-2-ylidene,[41] and 1,1,3,3-tetrakis(trimethylsilyl)dimethyltrisilan-1,3-diyldipotassium[21] were prepared according to literature procedures. The synthesis of $GeBr_2$·dioxane was carried out following the procedure for $GeCl_2$·dioxane[62] using $GeBr_4$.

2-Germa-1,1,3,3-tetrakis(trimethylsilyl)tetramethylcyclopentasilan-2-ylenetitanocene·PEt_3 Complex (2). *Method A.* Titanocene dichloride (55 mg, 0.22 mmol), **1** (131 mg, 0.20 mmol), and magnesium turnings (20 mg, 0.88 mmol) were suspended in THF (3 mL). The red suspension darkened upon sonification for 3 h and was further stirred for an additional 14 h at rt. The solvent of the dark blue suspension was removed under reduced pressure, and the residue extracted with pentane (3 times with 5 mL each). The volume of the dark violet extract was reduced to ca. 3 mL and stored at −35 °C. Dark violet to black crystals of **2** (65 mg, 39%) were obtained.

Method B. Starting compound **1** (328 mg, 0.50 mmol) and $Cp_2Ti(btmsa)$ (174 mg, 0.50 mmol) were dissolved in benzene (5 mL). The dark orange solution was warmed to 60 °C. After 2 h all volatiles were removed under reduced pressure. The residue was recrystallized from benzene (ca. 1 mL). A 190 mg (46%) amount of a dark violet to black crystalline **2** was obtained, mp 200−203 °C (dec). ^1H NMR (δ ppm, rt): 5.26 (s, 10H, Cp), 1.11 (s, 6H, PCH_2), 0.56 (bs, 57H, $SiMe_3$, $SiMe_2$, PCH_2CH_3). ^1H NMR (δ ppm, 50 °C): 5.28 (s, 10H, Cp), 1.16 (m, 6H, PCH_2), 0.65 (m, 9H, PCH_2CH_3), 0.54 (s, 36H, $SiMe_3$), 0.49 (s, 12H, $SiMe_2$). ^{13}C NMR (δ ppm, rt): 98.5 (Cp), 22.2 (PCH_2), 9.2 (PCH_2CH_3), 5.6 ($SiMe_3$), −0.5 ($SiMe_2$). ^{13}C NMR (δ ppm, 50 °C): 98.6 (Cp), 22.2 (PCH_2), 9.2 (PCH_2CH_3), 5.7 ($SiMe_3$), −0.4 ($SiMe_2$). ^{29}Si NMR (δ ppm, rt): −7.9 ($SiMe_3$), −24.9 ($SiMe_2$), −98.1 (Ti*Si*). ^{29}Si NMR (δ ppm, 50 °C): −6.2 ($SiMe_3$), −24.8 ($SiMe_2$), −97.1 (Ge*Si*). ^{31}P NMR (δ ppm, rt): 42.9. ^{31}P NMR (δ ppm, 50 °C): 41.6. UV absorption: λ_1 = 288 nm ($\varepsilon_1 = 1.2 \times 10^4$ [M^{-1} cm^{-1}]; shoulder); λ_2 = 340 nm ($\varepsilon_2 = 1.4 \times 10^4$ [M^{-1} cm^{-1}]); λ_3 = 531 nm ($\varepsilon_3 = 1.3 \times 10^3$ [M^{-1} cm^{-1}]). Anal. Calcd for $C_{32}H_{73}GePSi_8Ti$ (834.09): C 46.08, H 8.82. Found: C 43.84, H 8.77.

2-Germa-1,1,3,3-tetrakis(trimethylsilyl)tetramethylcyclopentasilan-2-ylenetitanocene·ImMe$_4$NHC Complex (2a). Complex **2** (250 mg, 0.30 mmol) and 1,3,4,5-tetramethylimidazol-2-ylidene (37 mg, 0.30 mmol) were dissolved in benzene (2 mL), and the dark violet solution was stirred at rt for 2 h. Then the solvent was removed under vacuum, and the dark violet residue was dissolved in pentane/toluene, filtered through glass wool, concentrated to a volume of about 0.5 mL, and stored at −35 °C. A dark violet waxy solid of **2a** was obtained (65 mg, 39%). ^1H NMR (δ ppm): 5.39 (s, 10H, Cp), 3.60 (s, 3H, N*Me*), 2.41 (s, 3H, N*Me*), 1.36 (s, 3H, C*Me*), 1.25 (s, 3H, C*Me*), 0.65 (s, 6H, $SiMe_2$), 0.61 (s, 18H, $SiMe_3$), 0.54 (s, 6H, $SiMe_2$), 0.51 (s, 18H, $SiMe_3$). ^{13}C NMR (δ ppm): 198.2 (Ti*C*), 125.5 (*C*Me), 124.8 (*C*Me), 99.4 (Cp), 42.2 (N*Me*), 34.2 (N*Me*), 9.5 (C*Me*), 8.7 (C*Me*), 5.4 ($SiMe_3$), 5.0 ($SiMe_3$), −0.4 ($SiMe_2$), −0.5 ($SiMe_2$). ^{29}Si NMR (δ ppm): −5.8 ($SiMe_3$), −7.3 ($SiMe_3$), −24.4 ($SiMe_2$), −100.4 (Ge*Si*).

2-Germa-1,1,3,3-tetrakis(trimethylsilyl)tetramethylcyclopentasilan-2-ylenezirconocene·PEt_3 Complex (3). Reaction was done according to method A using **1** (131 mg, 0.20 mmol), zirconocene dichloride (64 mg, 0.22 mmol), and magnesium turnings (20 mg, 0.88 mmol). Dark red crystals (96 mg, 55%) of **3** were obtained, mp 171−176 °C (dec). ^1H NMR (δ ppm): 5.43 (d, $^3J_{P,H}$ = 1.2 Hz, 10H, Cp), 1.07 (m, 6H, PCH_2), 0.63 (m, 9H, PCH_2CH_3), 0.62 (s, 18H, $SiMe_3$), 0.60 (s, 6H, $SiMe_2$), 0.51 (s, 18H, $SiMe_3$), 0.49 (s, 6H, $SiMe_2$). ^{13}C NMR (δ ppm): 98.9 (Cp), 19.7 (d, $^1J_{C,P}$ = 15.7 Hz, PCH_2), 8.1 (d, $^2J_{C,P}$ = 2.6 Hz, PCH_2CH_3), 5.0 ($SiMe_3$), 4.8 ($SiMe_3$), −0.9 ($SiMe_2$), −1.1 ($SiMe_2$). ^{29}Si NMR (δ ppm): −6.6 (d, $^4J_{P,Si}$ = 2.5 Hz, $SiMe_3$), −7.7 (d, $^4J_{P,Si}$ = 4.0 Hz, $SiMe_3$), −23.9 ($SiMe_2$), −100.7 (d, $^3J_{P,Si}$ = 2.1 Hz, Ge*Si*). ^{31}P NMR (δ ppm): 31.0. UV absorption: λ_1 = 302 nm ($\varepsilon_1 = 9.5 \times 10^3$ [M^{-1} cm^{-1}]; shoulder); λ_2 = 400 nm ($\varepsilon_2 = 2.3 \times 10^3$ [M^{-1} cm^{-1}]); λ_3 = 507 nm ($\varepsilon_3 = 7.0 \times 10^3$ [M^{-1} cm^{-1}]). Anal. Calcd for $C_{32}H_{73}GePSi_8Zr$ (877.44): C 43.80, H 8.39. Found: C 43.87, H 8.48.

2-Germa-1,1,3,3-tetrakis(trimethylsilyl)tetramethylcyclopentasilan-2-ylenehafnocene·PEt_3 Complex (4). Reaction was done according to method A using **1** (131 mg, 0.20 mmol), hafnocene dichloride (84 mg, 0.22 mmol), and magnesium turnings (20 mg, 0.88 mmol), yielding dark red crystals of **4** (103 mg, 53%), mp 173−177 °C (dec). ^1H NMR (δ ppm): 5.33 (s, 10H, Cp), 1.16 (m, 6H, PCH_2), 0.64 (m, 9H, PCH_2CH_3), 0.63 (s, 18H, $SiMe_3$), 0.62 (s, 6H, $SiMe_2$), 0.51 (s, 24H, $SiMe_3$, $SiMe_2$). ^{13}C NMR (δ ppm): 97.8 (Cp), 21.7 (d, $^1J_{C,P}$ = 18.9 Hz, PCH_2), 9.0 (d, $^2J_{C,P}$ = 2.8 Hz, PCH_2CH_3), 5.4 ($SiMe_3$), −0.4($SiMe_3$), −0.6($SiMe_3$). ^{29}Si NMR (δ ppm): −6.0 (d, $^4J_{Si,P}$ = 2.6 Hz, $SiMe_3$), −7.5 (d, $^4J_{Si,P}$ = 3.8 Hz, $SiMe_3$), −23.1 ($SiMe_2$), −101.8 (d, $^3J_{Si,P}$ = 2.9 Hz, Ge*Si*). ^{31}P NMR (δ ppm): 28.4. UV absorption: λ_1 = 294 nm ($\varepsilon_1 = 1.5 \times 10^4$ [M^{-1} cm^{-1}]; shoulder); λ_2 = 382 nm

dx.doi.org/10.1021/om400215v | *Organometallics* 2013, 32, 3300−3308

($\varepsilon_2 = 2.3 \times 10^3$ [M^{-1} cm^{-1}]); $\lambda_3 = 502$ nm ($\varepsilon_3 = 1.5 \times 10^4$ [M^{-1} cm^{-1}]). Anal. Calcd for $C_{32}H_{78}GeHfPSi_8$ (964.71): C 39.84, H 7.63. Found: C 38.69, H 7.58.

2-Germa-1,1,3,3-tetrakis(trimethylsilyl)-4,4-dimethylcyclotetrasilan-2-ylene·ImMe$_4$NHC Complex (5). A solution of 1,1,3,3-tetrakis(trimethylsilyl)dimethyltrisilan-1,3-diyldipotassium (1.00 mmol) in DME (10 mL) was slowly added to a vigorously stirred solution of $GeBr_2$·dioxane (236 mg, 1.05 mmol) and 1,3,4,5-tetramethylimidazol-2-ylidene (130 mg, 1.05 mmol) in 10 mL of DME at −30 °C. The dark red solution was stirred at rt for 14 h before the solvent was removed under reduced pressure. The orange-red residue was treated with pentane (3 times with 5 mL each). The volume of the extract was reduced to ca. 3 mL and stored at −35 °C. An orange solid of **5** (440 mg, 73%) was obtained. ^{1}H NMR (δ ppm, rt): 3.30 (s, 6H, N*Me*), 1.21 (s, 6H, C*Me*), 0.75 (s, 6H, Si*Me*$_2$), 0.46 (s, 36H, Si*Me*$_3$). ^{1}H NMR (δ ppm, 60 °C): 3.30 (s, 6H, N*Me*), 1.31 (s, 6H, C*Me*), 0.74 (s, 6H, Si*Me*$_2$), 0.45 (s, 36H, Si*Me*$_3$). ^{13}C NMR (δ ppm, rt): 177.4 (GeC), 124.8 (*C*Me), 34.8 (N*Me*), 8.2 (C*Me*), 5.6 (Si*Me*$_3$), 3.7 (Si*Me*$_2$). ^{13}C NMR (δ ppm, 60 °C): 178.5 (GeC), 125.2 (*C*Me), 35.3 (N*Me*), 8.5 (C*Me*), 6.0 (Si*Me*$_3$), 4.0 (Si*Me*$_2$). ^{29}Si NMR (δ ppm, rt): −17.8 (*Si*Me$_2$), −103.5 (Ge*Si*). ^{29}Si NMR (δ ppm, 60 °C): −9.3 (*Si*Me$_3$), −17.3 (*Si*Me$_2$), −102.1 (Ge*Si*). Anal. Calcd for $C_{21}H_{54}GeN_2Si_7$ (603.91): C 41.77, H 9.01, N 4.64. Found: C 41.27, H 8.96, N 4.99.

2-Germa-1,1,3,3-tetrakis(trimethylsilyl)dimethylcyclotetrasilan-2-ylenetitanocene·ImMe$_4$NHC Complex (6). Starting material **5** (121 mg, 0.20 mmol) and Cp_2Ti(btmsa) (70 mg, 0.20 mmol) were dissolved in benzene (3 mL). The dark green suspension was stirred for 24 h at 60 °C before the solvent of the dark blue suspension was removed under reduced pressure. The residue was dissolved in pentane (5 mL) and stored at −35 °C. Dark violet crystals of **6** were obtained (120 mg, 77%), mp 223−233 °C (dec). ^{1}H NMR (δ ppm): 5.34 (s, 10H, Cp), 3.71 (s, 3H, N*Me*), 2.39 (s, 3H, N*Me*), 1.28 (s, 3H, C*Me*), 1.24 (s, 3H, C*Me*), 0.80 (s, 3H, Si*Me*), 0.75 (s, 3H, Si*Me*), 0.66 (s, 18H, Si*Me*$_3$), 0.52 (s, 18H, Si*Me*$_3$). ^{13}C NMR (δ ppm): 197.6 (Ti*C*), 125.4 (*C*Me), 124.7 (*C*Me), 99.1 (Cp), 42.2 (N*Me*), 33.9 (N*Me*), 9.4 (*C*Me), 8.6 (*C*Me), 5.3 (Si*Me*$_3$), 5.2 (Si*Me*$_3$), 4.6 (Si*Me*), 4.3 (Si*Me*). ^{29}Si NMR (δ ppm): −8.4 (*Si*Me$_3$), −8.7 (*Si*Me$_3$), −18.0 (*Si*Me$_2$), −68.7 (Ge*Si*).

■ ASSOCIATED CONTENT

Supporting Information

NMR spectra of compounds **2** and **4**, crystallographic data for compounds **2**, **3**, **4**, and **6** in a table and in CIF format as well as details of the theoretical studies are available free of charge via the Internet at http://pubs.acs.org.

■ AUTHOR INFORMATION

Corresponding Author

*E-mail: baumgartner@tugraz.at, christoph.marschner@tugraz.at, thomas.mueller@uni-oldenburg.de.

Author Contributions

The manuscript was written through contributions of all authors. All authors have given approval to the final version of the manuscript.

Notes

The authors declare no competing financial interest.

■ ACKNOWLEDGMENTS

Support for this study was provided by the Austrian Fonds zur Förderung der Wissenschaftlichen Forschung (FWF) via the projects P-19338, P-22678, and P-25124. P.Z. thanks the Fonds der Chemischen Industrie (FCI) for a scholarship (No. 183191). The High-Performance Computing Center (HERO) of the CvO University is thanked for computer time. The authors are grateful to Prof. Hans-Jörg Weber (TU Graz) for help with NOE experiments.

■ REFERENCES

(1) Petz, W. *Chem. Rev.* **1986**, *86*, 1019−1047.
(2) Lappert, M. F.; Rowe, R. S. *Coord. Chem. Rev.* **1990**, *100*, 267−292.
(3) Leung, W.-P.; Kan, K.-W.; Chong, K.-H. *Coord. Chem. Rev.* **2007**, *251*, 2253−2265.
(4) Asay, M.; Jones, C.; Driess, M. *Chem. Rev.* **2011**, *111*, 354−396.
(5) Sharma, H. K.; Haiduc, I.; Pannell, K. H. In *The Chemistry of Organic Germanium, Tin and Lead Compounds Vol. 2*; Rappoport, Z., Ed.; John Wiley & Sons, Ltd: Chichester, 2002; Vol. 2, pp 1241−1332.
(6) Zirngast, M.; Flock, M.; Baumgartner, J.; Marschner, C. *J. Am. Chem. Soc.* **2009**, *131*, 15952−15962.
(7) Fischer, J.; Baumgartner, J.; Marschner, C. *Organometallics* **2005**, *24*, 1263−1268.
(8) Woo, H. G.; Freeman, W. P.; Tilley, T. D. *Organometallics* **1992**, *11*, 2198−2205.
(9) Ovchinnikov, Y. E.; Igonin, V.; Timofeeva, T. V.; Lindeman, S. V.; Struchkov, Y. T.; Ustinov, M. V.; M., V.; Bravo-Zhivotovskii, D. A. *Metalloorg. Khim.* **1992**, *5*, 1154−1160.
(10) Ermolaev, N. L.; Borisova, Z. K.; Kosyak, A. M.; Kochnev, N. V. *Metalloorg. Khim.* **1990**, *3*, 553−555.
(11) Aitken, C.; Harrod, J. F.; Malek, A.; Samuel, E. *J. Organomet. Chem.* **1988**, *349*, 285−291.
(12) Arnold, J.; Roddick, D. M.; Tilley, T. D.; Rheingold, A. L.; Geib, S. J. *Inorg. Chem.* **1988**, *27*, 3510−3514.
(13) Harrod, J. F.; Malek, A.; Rochon, F. D.; Melanson, R. *Organometallics* **1987**, *6*, 2117−2120.
(14) Roesch, L.; Altnau, G.; Erb, W.; Pickardt, J.; Bruncks, N. *J. Organomet. Chem.* **1980**, *197*, 51−57.
(15) Razuvaev, G. A.; Vyshinskaya, L. I.; Vasil'eva, G. A.; Latyaeva, V. N.; Timoshenko, S. Y.; Ermolaev, N. L. *Izv. Akad. Nauk SSSR, Ser. Khim.* **1978**, 2584−2588.
(16) Razuvaev, G.; Latyaeva, V. N.; Vishinskaya, L. I.; Bytchkov, V. T.; Vasilyeva, G. A. *J. Organomet. Chem.* **1975**, *87*, 93−99.
(17) Razuvaev, G. A.; Latyaeva, V. N.; Vasil'eva, G. A.; Vyshinskaya, L. I. *Izv. Akad. Nauk SSSR, Ser. Khim.* **1972**, 1658−1659.
(18) Kingston, B. M.; Lappert, M. F. *J. Chem. Soc., Dalton Trans.* **1972**, 69−73.
(19) During the 16th International Symposium on Silicon Chemistry (ISOS XVI), August 14−18, 2011, in Hamilton, Canada, some of the results covered in this article were the subject of an oral presentation. At the same conference Dr. Vladimir Ya. Lee (University of Tsukuba, Japan) reported on related chemistry utilizing the reaction of metallocene dichlorides with geminal germanium dianions.
(20) Kayser, C.; Kickelbick, G.; Marschner, C. *Angew. Chem., Int. Ed.* **2002**, *41*, 989−992.
(21) Fischer, R.; Frank, D.; Gaderbauer, W.; Kayser, C.; Mechtler, C.; Baumgartner, J.; Marschner, C. *Organometallics* **2003**, *22*, 3723−3731.
(22) Arp, H.; Baumgartner, J.; Marschner, C.; Zark, P.; Müller, T. *J. Am. Chem. Soc.* **2012**, *134*, 6409−6415.
(23) Arp, H.; Baumgartner, J.; Marschner, C.; Müller, T. *J. Am. Chem. Soc.* **2011**, *133*, 5632−5635.
(24) Hlina, J.; Baumgartner, J.; Marschner, C.; Albers, L.; Müller, T. *Organometallics* **2013**, accepted.
(25) Arp, H.; Baumgartner, J.; Marschner, C.; Zark, P.; Müller, T. *J. Am. Chem. Soc.* **2012**, *134*, 10864−10875.
(26) Whittal, R. M.; Ferguson, G.; Gallagher, J. F.; Piers, W. E. *J. Am. Chem. Soc.* **1991**, *113*, 9867−9868.
(27) Piers, W. E.; Whittal, R. M.; Ferguson, G.; Gallagher, J. F.; Froese, R. D. J.; Stronks, H. J.; Krygsman, P. H. *Organometallics* **1992**, *11*, 4015−4022.
(28) Bares, J.; Richard, P.; Meunier, P.; Pirio, N.; Padelkova, Z.; Cernosek, Z.; Cisarova, I.; Ruzicka, A. *Organometallics* **2009**, *28*, 3105−3108.
(29) Blom, B.; Driess, M.; Gallego, D.; Inoue, S. *Chem.—Eur. J.* **2012**, *18*, 13355−13360.
(30) Lee, V. Y.; Aoki, S.; Yokoyama, T.; Horiguchi, S.; Sekiguchi, A.; Gornitzka, H.; Guo, J.-D.; Nagase, S. *J. Am. Chem. Soc.* **2013**, *135*, 2987−2990.

(31) Nakata, N.; Fujita, T.; Sekiguchi, A. *J. Am. Chem. Soc.* **2006**, *128*, 16024−16025.
(32) Burlakov, V. V.; Polyakov, A. V.; Yanovsky, A. I.; Struchkov, Y. T.; Shur, V. B.; Vol'pin, M. E.; Rosenthal, U.; Görls, H. *J. Organomet. Chem.* **1994**, *476*, 197−206.
(33) Rosenthal, U.; Ohff, A.; Michalik, M.; Görls, H.; Burlakov, V. V.; Shur, V. B. *Angew. Chem.* **1993**, *105*, 1228−1230.
(34) Hlina, J. Ph.D. thesis, Technische Universität Graz, Graz, 2013.
(35) Ohff, A.; Pulst, S.; Lefeber, C.; Peulecke, N.; Arndt, P.; Burkalov, V. V.; Rosenthal, U. *Synlett* **1996**, *1996*, 111−118.
(36) Rosenthal, U.; Burlakov, V. V.; Arndt, P.; Baumann, W.; Spannenberg, A. *Organometallics* **2003**, *22*, 884−900.
(37) Niehues, M.; Erker, G.; Kehr, G.; Schwab, P.; Fröhlich, R.; Blacque, O.; Berke, H. *Organometallics* **2002**, *21*, 2905−2911.
(38) Baker, R. J.; Bannenberg, T.; Kunst, A.; Randoll, S.; Tamm, M. *Inorg. Chim. Acta* **2006**, *359*, 4797−4801.
(39) Büschel, S.; Bannenberg, T.; Hrib, C. G.; Glöckner, A.; Jones, P. G.; Tamm, M. *J. Organomet. Chem.* **2009**, *694*, 1244−1250.
(40) Marsh, R. E. *Acta Crystallogr. B* **1997**, *53*, 317−322.
(41) Kuhn, N.; Kratz, T. *Synthesis* **1993**, 561−562.
(42) The Gaussian 09 program was used. *Gaussian 09* Revision B.01; Gaussian, Inc.: Wallingford, CT, 2010. For a detailed description of the computations, see the Supporting Information.
(43) Details of these computed structures are discussed elsewhere; see ref 24.
(44) The dihedral angle β is defined by the EMP and the SiESi planes in the monotetrylene complexes.
(45) Pyykkö, P.; Atsumi, M. *Chem.—Eur. J.* **2009**, *15*, 12770−12779.
(46) Kaupp, M. *J. Comput. Chem.* **2007**, *28*, 320−325.
(47) Buijse, M. A.; Baerends, E. J. *J. Chem. Phys.* **1990**, *93*, 4129−4141.
(48) Li, J.; Schreckenbach, G.; Ziegler, T. *Inorg. Chem.* **1995**, *34*, 3245−3252.
(49) Li, J.; Ziegler, T. *Organometallics* **1996**, *15*, 3844−3849.
(50) Zark, P. Ph.D. thesis, Universität Oldenburg, Oldenburg, 2012.
(51) Zhao, Y.; Truhlar, D. G. *Theor. Chem. Acc.* **2007**, *120*, 215−241.
(52) Sieffert, N.; Bühl, M. *Inorg. Chem.* **2009**, *48*, 4622−4624.
(53) Schreiner, P. R.; Chernish, L. V.; Gunchenko, P. A.; Tikhonchuk, E. Y.; Hausmann, H.; Serafin, M.; Schlecht, S.; Dahl, J. E. P.; Carlson, R. M. K.; Fokin, A. A. *Nature* **2011**, *477*, 308−311.
(54) Grimme, S.; Schreiner, P. R. *Angew. Chem., Int. Ed.* **2011**, *50*, 12639−12642.
(55) Pangborn, A. B.; Giardello, M. A.; Grubbs, R. H.; Rosen, R. K.; Timmers, F. J. *Organometallics* **1996**, *15*, 1518−1520.
(56) Morris, G. A.; Freeman, R. *J. Am. Chem. Soc.* **1979**, *101*, 760−762.
(57) Helmer, B. J.; West, R. *Organometallics* **1982**, *1*, 877−879.
(58) *SAINTPLUS: Software Reference Manual*, Version 6.45; Bruker-AXS: Madison, WI, USA, 1997−2003.
(59) Sheldrick, G. M. *SADABS*, Version 2.10; Bruker AXS Inc.: Madison, WI, USA, 2003.
(60) Blessing, R. H. *Acta Crystallogr. A* **1995**, *51*, 33−38.
(61) Sheldrick, G. M. *Acta Crystallogr. A* **2007**, *64*, 112−122.
(62) Leigh, W. J.; Harrington, C. R.; Vargas-Baca, I. *J. Am. Chem. Soc.* **2004**, *126*, 16105−16116.